Particles Motion in a Cascading Rotary Drum Dryer

Ihsan Hamawand* and Talal Yusaf

National Centre for Engineering in Agriculture (NCEA), Faculty of Engineering and Surveying, University of Southern Queensland, Toowoomba, 4350 QLD, Australia

A mathematical model was built and used to show the motion of particles in a cascade rotary drum dryer. In a cascade rotary drum the flights pick up the particles at a number of points in the lower half of the drum while, in the upper half, the particles fall freely. A model is derived where the drag force exerted on the particles throughout the falling period is emphasised. The motion of the particles in a rotary drum is described by three actions: Cascade; Kiln and Bouncing. In this study a horizontal rotary drum was used where both the kiln and bouncing actions have minimal effect, therefore, the focus is on the cascade motion of the particles. A characteristic of the model is the "falling number" which is found to be dependent on the curtain properties. The model has demonstrated its ability to predict the effect of many important parameters such as drying medium velocity, drum rotation speed, particle size and feeding flow rate. It has been shown that increasing the drying medium velocity by 2.5 times results in an 85% decrease in the residence time. Also, the number of falling is shown to be limited and a function of the drum rotation speed, in this case 0.59 falling per second. An important feature of this model is the ability to predict the mean resident time, contact time interval and the resting time interval. The maximum error between the predicted and the measured data was <10%.

Keywords: rotary drum, mathematical model, particle motion, particle drag, cascade motion, residence time

INTRODUCTION

A rotary cascaded dryer is one of the many unit operations that have been used in industry. In most drying applications, the drying medium and the feeding of the solids are flows co-currently through the dryer. Co-current feeding is preferred because it reduces the thermal degradation of the product, especially for heat sensitive materials. In this case, the axial movement of the solids is aided by both the slope of the dryer and the drag force acting on the cascading particles. Most of the drying occurs while the particles are falling into the gas–solids contact space. The importance of the residence time in the rotary drum is due to its effect on both heat and mass transfer; both of which are the main factors for successful design. The time interval of contact with the inlet gas and axial position in the drum are very important variables for the heat transfer calculations because the drying medium changes temperature axially through the drum.

Modelling the particle motion in a rotary drum has been a challenge because of the many variables that affect particles displacement through the drum. There has been a reliance on empirical equations to estimate the mean residence time of the particles. However, empirical models are only applicable to specific circumstances and their generalisation is limited.

Song et al.[1] evaluated several empirical design correlations to predict the average residence time in the rotary dryer. Song showed that out of three correlations: Perry and Green,[2] Foust et al.[3] and Friedman and Marshal,[4] the correlation given by Perry and Green[2] was the most accurate. However, the residence time predictions using the Perry & Green[2] correlation were too high. In another study by Renaud et al.,[5] they developed a model for an industrial rotary dryer. Renaud used the modified Cholette–Cloutier model first presented by Duchesne et al.[6] Renaud did a comparison with many empirical correlations, including Sullivan et al.,[7] Friedman and Marshal,[4] Faust et al.,[3] Perry et al.,[2] Sai et al.[8] and Alvarez and Shene.[9] The comparisons showed a good agreement between the experiment with the simulated model and the modified Cholette–Cloutier model. However, there was a great discrepancy between the other empirical correlations and the experimental data. Furthermore, Shahhosseini[10] showed in his study that a simple semi-empirical model of Freidman and Marshal with some modification can predict solid hold-up and flow rate with reasonable accuracy in some circumstances. Moreover, Kemp[11] had summarised some correlations and models of particle motion in cascading rotary dryers in his paper and reformulated the model of Matchett and Baker[12] into a semi-empirical correlation. However, Cao and Langrish[13] found that the model of Matchett and Baker gives more satisfactory solid residence time predictions in pilot scale and full scale industries rotary dryers. In their experiments, the slopes were 4.5° and above, larger than those in the industrial scale coolers and dryers. From the above studies it is obvious that many of these empirical correlations have been developed for specific circumstances and their application cannot be generalised. A number of mechanistic solid transport models were presented by Kelly and O'Donnell,[14] Baker[15] and Wang et al.[16] These models calculate the particles' axial displacement by considering the geometry of the rotating flights. As described by Shahhosseini,[10] these models are heavily dependent on empirical correlations and are not fully mechanistic, and when tested by Earner[17] were found to be inaccurate. Furthermore, Sheehan[18] and Britton et al.[19] developed a predominantly mechanistic model for solid transport in a flighted rotary dryer. The model combined conventional reactor compartment modelling with geometric flight analysis. Their model predicted the residence time distribution (RTD) based on dryer geometry and material properties. They show the effect of drum rotation speed, diameter scaling, and the

*Author to whom correspondence may be addressed.
E-mail address: ihsan.hamawand@usq.edu.au
Can. J. Chem. Eng. 92:648–662, 2014

DOI 10.1002/cjce.21845
Published online 29 July 2013 in Wiley Online Library (wileyonlinelibrary.com).

number of flights on the residence time distribution in an industrial sugar dryer. However, in their work the effect of gas-particle drag was determined through parameter estimation rather than a completely mechanistic determination of the effects of particle drag.

The effect of air flow on the particle transport through a cascading rotary dryer is the focus of the present study. Baker[15] studied this variable theoretically and experimentally by formulating two models. In the first model the drag coefficient between air and a particle is calculated on the assumption of a single spherical particle, while in the second model, the drag coefficient was calculated for a curtain of particles. However, the study by Baker did not cover the most effective variable in a cascade rotary drum dryer. The aim of the present study is to develop an analytical model that emphasises the impact of the gas flow rate on the axial displacement of the particles through a flighted rotary drum. In this model, many variables that affect the residence time of the particles have been included. In addition to performing experiments, the predictions of the model were compared to published data. The model is capable of estimating the average time that a particle spends in contact with the drying medium and the time particles spent in rest or 'equilibration.' Furthermore, the model determines the axial position of a particle with time. The innovation in this paper is the determination of the 'falling number'; the average number of times a particle will fall freely accounting for the effect of rotation speed of the drum, feed flow rate, diameter of the drum, number of flight, the curtain of particles properties, and gas inlet velocity.

MODEL

Particle Motion Behaviour

Particles' movement along the axis of a flighted rotary drum is controlled by three motions: (a) the particles are swept by the gas as they fall from the flights (cascade); (b) the particles roll along the dryer base (kiln action) and (c) the particles bound off the dryer surface (bouncing). A Kiln action is the motion of particles as they slide down the metal surfaces in the lower half of the shell, or as they slide over one another. The kiln action phenomenon in the axial direction is due to the slope of the dryer and the hydraulic gradient in an over-loaded drum. The drum is over-loaded when the feed cannot be retained by the flights, in other words, the feed materials freely move over the flights. The experimental data of Kelly and O'Donnell[20] showed that the Kiln action was of major importance in an overloaded dryer. In spite the importance of Kiln in the over-loaded condition, it only accounts for less than 10% of the axial motion of the particles.[21] Bouncing motion occurs when falling particles rebound from the metal surface when they reach the ground surface of the drum. It was also shown by Kelly and O'Donnell[20] that bouncing has a major effect in under-loaded drums. This is when a small amount of feed is presented in the drum which allows a larger contact region between the feed and the lower metal-base of the drum. The last action is the Cascade motion. Cascade results from the lifting action of the flights in a rotating drum and entrainment of these particles in the gas stream. In a horizontal drum the falling particles are mostly displaced axially due to the drag force of the inlet gas. In an inclined drum they are displaced axially due to the drum slope as well.

Height and Angle of Discharge of the Flights

For a non-overloaded horizontal drum (zero slope), the entrainment action is the most important factor that controls the axial velocity of the particles along the drum. The purpose of the flights is to accumulate particles in order to prevent them rolling down inside the wall of the drum. However, this accumulation process means that there is more than one particle held by the flight and therefore the particles are discharged over a period rather than a point in time. Figure 2 shows the cross-section of a rotating drum fitted with four flights. ϕ is the angle of rotation around the drum axis with $\phi = 0$ when the flight is in the 3 O'clock position. In their studies, Pan et al.[22] showed that for an inclined flighted drum the initial angle of discharge was $\phi \geq 0$ for an under-loaded flight and $\phi < 0$ for an over loaded flight. The finishing discharges for both are around $\phi \geq \pi/2$.

Thus for under or a design loaded drum (the cumulative materials at the base of the drum are lower or at the same level of the flight) the following simple Equation (1) presented by Kelly and O'Donnell[23] for EAD (Equal Angular Distribution) flights can be used. Equation (1) predicts the average vertical distance travelled by a particle to reach the drum floor. However, the EAD flights and the flights in this study (see the appendix) are not precisely similar, the average vertical travelling distance of the particles are quite alike when the calculated value from Equation (1) is compared with the observed from the experiments.

$$H = \frac{2\bar{D}}{\pi \cos\varphi} \tag{1}$$

The equation above assumes a vertical path of the particles when there is no gas flow where H is the average length of fall, $\bar{D}$ is the effective diameter of the drum $[\bar{D} = D - s]$, and φ is the slope of the drum, for a horizontal dryer $[\cos\varphi = 1]$, s is the length of the retainer on each flight.

Horizontal Displacement of Particles

As stated by Vincent[24], Walton provided a definitive scientific description of particle elutriation in air flows which is still accepted to this date. The theory is based on the settling behaviour of particles which is controlled by gravitational settling.

The horizontal displacement of the particles in the x-axis direction, when there is gas flow co-current to the solid feed, was calculated using Equation (2) represented by Walton in 1954.

$$\frac{x / v_{\mathrm{p}}}{H/V_{\mathrm{ts}}} = 1 \tag{2}$$

$$x = \frac{H\ v_{\mathrm{p}}}{V_{\mathrm{ts}}} \tag{3}$$

where H is the average length of fall, V_{ts} is the terminal velocity of the particles and v_{p} is the velocity of the particles in the axial direction due to drag force exerted by the fluid motion through the rotary drum.

The terminal velocity for a single particle can be calculated according to the particle and the gas inlet properties. Assuming that the vertical drag is negligible as was shown by Kelly and O'Donnell,[14] the balance of the force in the Cartesian x-axis direction is presented in Equation (4):

$$m_{\mathrm{p}} \frac{\mathrm{d}v_{\mathrm{p}}}{\mathrm{d}t} = 0.5 C_D \rho_g A_p (u - v_{\mathrm{p}})^2 \tag{4}$$

The analytical solution of Equation (4) is shown in Equation (5), assuming the axial velocity of the particle when it begins its fall is

zero ($v_p = 0$, at $t = 0$).

$$v_p = u - \frac{u}{\alpha\, ut + 1} \tag{5}$$

where u is the superficial gas inlet velocity and α is presented in Equation (6):

$$\alpha = \frac{0.5 C_D \rho_g A_p}{m_p} \tag{6}$$

Vertical Velocity of Particles

Koichiro et al.[25] measured the velocity of a powder jet falling from a hopper using a phase Doppler anemometer. They found that the velocity of the powder at the exit of the hopper is close to the free falling velocity of a single particle. Regardless of the fluid drag, the free falling velocity is independent of the diameter, density and mass flow rate of the particles and far from the exit tends to approach the terminal settling velocity of a single particle.

The average settling velocity of particles due to gravity in a falling curtain can be calculated using Equation (7). It is assumed that the vertical velocity of the particles reaches the terminal velocity of a single particle quickly because the particles are accelerated as they fall into the wake of the particles ahead. Although the effects of air drag on curtaining particles can be quantified or modelled using CFD (see for example Wardjamin et al.[26] and Lee[27]). For the sake of simplicity single particle drag is considered. Equations (8)–(10) describe the drag action in the model.

To account for the uncertainties in the description of the particles velocity in curtains, such as particles rolling before they fall from the flight and having non-zero initial vertical velocity, the density in Equation (7) is manipulated. The reasoning for this is that the main influence on whether a particle in a curtain reaches terminal velocity is considered to be the voidage or curtain density. For example, using the bulk density instead of the particle density in Equation (7), the average velocity of the curtain of particles is approximately 60% of the terminal velocity of a single particle. This is true when compared to the founding of Koichiro et al.[25] who they showed that particles reach terminal velocities only at the exit. This allows for the calculation of the average velocity of a single particle because not all the particles in the curtain will fall at the same time or with the same initial velocities. In addition, curtains behave differently to a single particle (Wardjamin et al.[26] and Lee[27]).

$$V_{ts} = \frac{\rho_p {d_p}^2 g}{18 \mu_g} \tag{7}$$

Assuming spherical particles, the mass of each particle is:

$$m_p = \frac{\pi}{6} {d_p}^3 \rho_p \tag{8}$$

The drag coefficient was calculated using the equation of Kaskas,[28] which is applicable over the range of particle Reynold number $0 < Re_p < 4 \times 10^5$.

$$C_D = \frac{24}{Re_p} + \frac{4}{\sqrt{Re_p}} + 0.4 \tag{9}$$

where the particle Reynold number is:

$$Re_p = \frac{\rho_g u\, d_p}{\mu_g} \tag{10}$$

Number of Times That Particles Are Elutriated Through the Drum

A new equation is developed (Equation 11) that estimates the number of times an average particle will fall from a flight to the base of the drum per unit time. This is defined as the falling number (N) per unit time and is a function of many variables as shown in Figure 1, such as the drum circumference (πD), the rotation speed in revolutions per second (rps), the number of flights (F_N), the feed mass flow rate (F), the feed hold-up (H_{up}), the diameter of the drum (D) and the terminal velocity of the particles (V_{ts}).

$$N = \frac{1}{\frac{\pi D/F_N}{2\pi D\,\mathrm{rps}} + \frac{\pi D/2}{\pi D\,\mathrm{rps}} + \frac{F\Delta t^2}{H_{up}} + \frac{H}{V_{ts}}} \tag{11}$$

where,

$\left[\frac{\pi D/2}{\pi D\,\mathrm{rps}}\right]$ Represents the average time interval from the beginning of lifting to the beginning of falling. The discharge region is between $0 < \phi < \pi/2$, see (term A) in Figure 4.

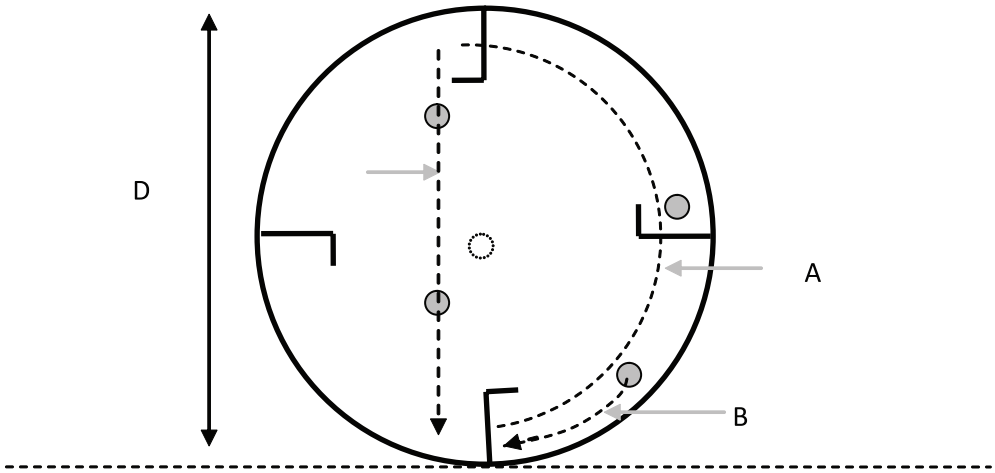

Figure 1. A schematic showing the terms in Equation (11).

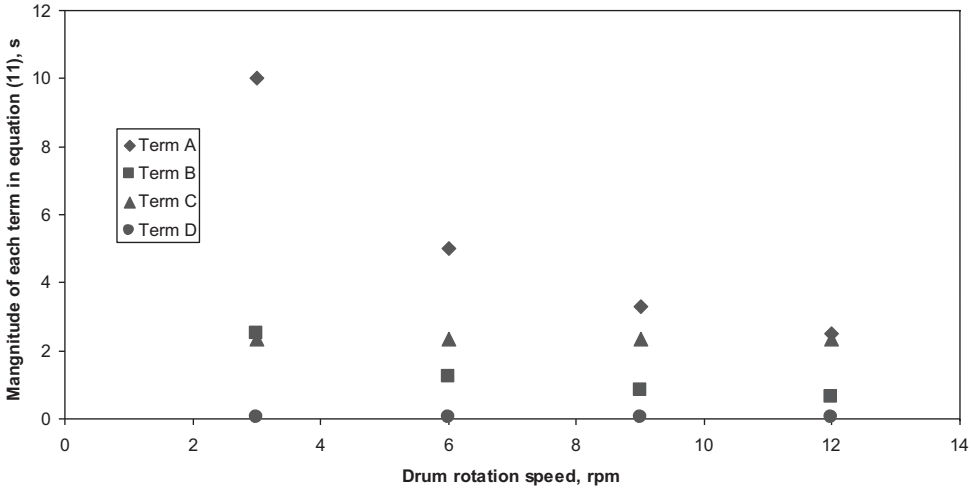

Figure 2. Comparison of the magnitude of each term in Equation (11) versus rotary drum speed at constant gas inlet velocity $U = 1$ m/s, $D = 0.37$ m, dp = 385 μm, $L = 3.0$ m, $F_N = 4$, $F = 1$ kg/min.

$\left[\frac{\pi D/F_N}{2\pi D\,\mathrm{rps}}\right]$ The average time for the particle to travel from the rear of one flight to the interior of the next one by sliding action, see (term B) in Figure 4.

$[F\,\Delta t^2/H_{up}]$ This term was included to introduce the effect of the loading, as the feed mass flow rate increases it may lead to an increase in the hold-up height above the flight's which may decrease the probability of the particle to be captured by the flight and fall, see (term C) in Figure 4. Δt is the unit time interval.

$[H/V_{ts}]$ Time interval for the particle to fall through the average distance H, see (term D) in Figure 4.

JUSTIFICATION OF THE TERMS IN THE NEW EQUATION (FALLING NUMBER)

Figures 2 and 3 are plotted to show the justification for each term in Equation (11). Figure 2 shows that both average travelling intervals for the particles between two flights (term B in Equation (11)) and from the beginning of lifting to beginning of falling (term A in Equation (11)) decreases as the drum speed increases. There is a significant decrease by 80% in the travelling time of the particle from the beginning of lifting to the beginning of falling as the drum speed increases from 3 to 12 rpm. This is due to the fact that the particles travel a shorter distance over the surface of the drum in the opposite direction to the drum rotation until it is captured by the flight, and then it is fixed at that point until it reaches the falling point so its speed is the same as the drum speed. Both the interval of falling (term D in Equation (11)) and the interval that a particle will take to be captured by the flight due to feed effect (term C in Equation (11)) are constant as long as the properties of the particles and the feed rate are constant. The interval of falling or the contact time between the particles and the gas inlet has the lowest magnitude of around 0.044 s. This is because each particle has a vertical velocity related to the curtain properties with an average of 60% of a single particle terminal velocity. However, while the time a particle spends in contact with the drying medium is small, it has the greatest effect on the drying of materials and its magnitude rises with the increases in drum rotation speed.

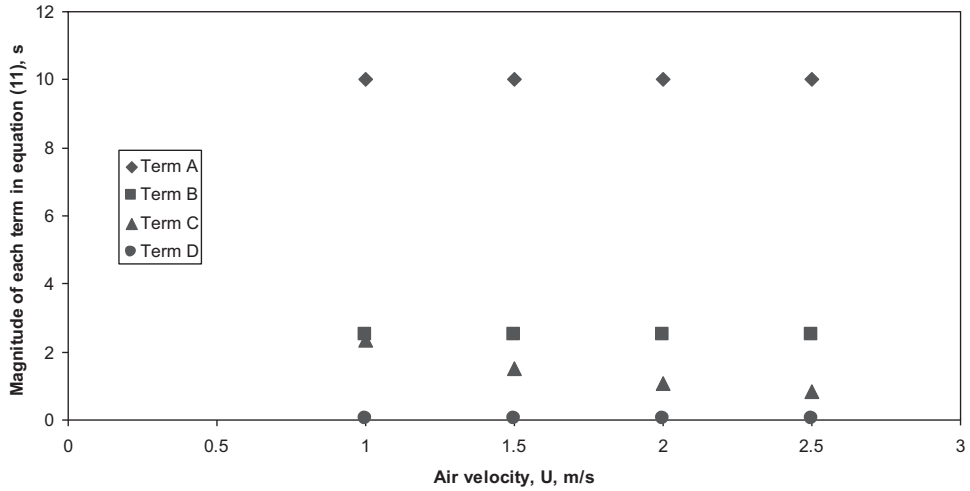

Figure 3. Comparison of the magnitude of each term in Equation (11) versus inlet gas velocity at constant drum rotation speed rpm = 3, $D = 0.37$ m, dp = 385 μm, $L = 3.0$ m, $F_N = 4$, $F = 1$ kg/min.

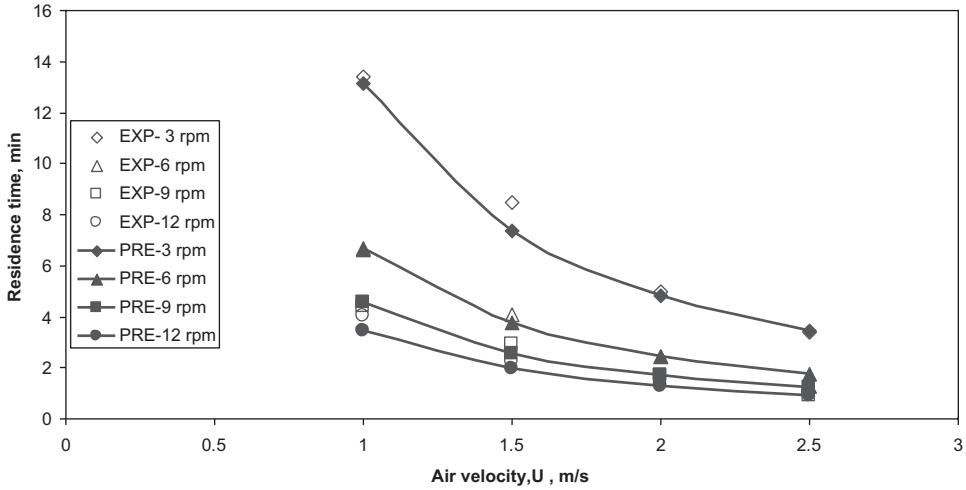

Figure 4. Comparison of the experimental results of this study with the suggested model versus gas inlet velocity at variable drum rotation speed, D = 0.37 m, dp = 385 μm, L = 3.0 m, $F_N = 4$, F = 1 kg/min.

At variable air velocity and constant drum speed rotation, as expected, both the travelling intervals for the particles from beginning of lifting to beginning of falling and between two flights are constant as shown in Figure 3. The only trend that changes is the interval that the particles will take to be captured by the flight due to feed effect (term C in Equation (11)). When the solid feed flow rate is constant, the graph shows that an increase in air velocity leads to a decrease in the interval that the particles will take to be captured by the flight. This is due to the decrease in the hold up as the residence time decreases.

CALCULATED DRUM HOLD-UP

Empirical equations for estimation of the drum hold up, which do not consider the gas flow rate, were proposed by Sai et al.[8] The hold-up was calculated locally for each displacement $[x_i]$ using Equation (12). Equation (12) represents the hold-up as function of the position of the particle during its displacement through the drum:

$$H_{up} = \rho_p x_i \left[\frac{D}{2}\right]^2 (\theta - \sin\theta)/2 \tag{12}$$

where H_{up} is the drum hold-up, x_i is the instantaneous displacement along the length of the drum, and θ is the angle of dispersion of the feed radially at the lower half of the shell. In other words, it is the cross sectional arc representing the amount of solid feed at the lower part of the shell.

The height of the solid in the drum (Equation 13) is assumed to be in the range of the flight height for a fully loaded design. Then the angle of solid dispersion (θ) in the lower half of the shell was calculated. From the observation and analysis of the video footage taken for the drum at different drum speeds[3–15] rpm, the feed rate used in the experiments was sufficient to not exceed the height of the flight(s).

$$s = h = \left[\frac{D}{2}\right]\left[1 - \cos\left(\frac{\theta}{2}\right)\right] \tag{13}$$

RESIDENCE TIME

The mean residence time of the particles in the drum τ can be estimated by dividing the drum length by the axial speed of the particles (Equation 14), where Nx represents the axial speed.

$$\tau = \frac{L}{Nx} \tag{14}$$

The time of contact between the particles and the gas inlet medium, which is the actual time of drying in a drying system can be calculated from Equation (15):

$$\tau_{contact} = N \frac{\left(x^2 + H^2\right)^{0.5}}{V_{ts}} \tau \tag{15}$$

The remaining time will be the rest time for the particles where they equilibrate their moisture content with the other particles in a drying drum which can be calculated using Equation (16):

$$\tau_{rest} = \tau - \tau_{contact} \tag{16}$$

SINGLE PARTICLE EFFECT

The modelling results show that Equation (14) is significantly affected by the particle sizes and properties through the term V_{ts} (Equation 7) and the term D in Equation (11). However, Koichiro et al.[25] showed that this is not true when dealing with a swamp of particles. It has been found that the residence time for a single particle is significantly further away from that measured experimentally and that predicted by the normalised effect of particle size. The residence time for the curtain of particles was measured (experimentally) to be around 13 min. However, for a single particle the residence time predicted by the model was close to 25 min. It seems that the drag force has a reduced effect on a curtain of particles as shown by Kemp[11] and Baker.[15] Even for a sloped drum, the particle size has a very little effect on the mean residence

time.[29] For this reason, an assumption was made to normalise the effect of the mean particle size of the curtain of particles in this study by introducing an effective particle size in Equation (17):

$$d_{pE}(\mu m) = 100 + c_1[d_p]^{c_2} \quad (17)$$

where d_{pE} is the effective particle diameter which used in the model equations, c_1 and c_2 are constant obtained by fitting Equation (17) to the experimental data ($c_1 = 0.05$ and $c_2 = 2.0$). The mean particle size was calculated for the material used in the experiments and it was 385 μm.

EXPERIMENTAL PROCEDURES

Drum Descriptions

A 3 m long pilot scale rotary drum dryer with a diameter of 0.37 m was used in this study. Commercial sand was used with a mean particle size of 385 μm and a bulk density of 1650 kg/m^3. A direct contact rotary drum with con-current flow of gas and solids was used. The rotary cylinder was made of stainless steel and both ends were sealed to prevent gas leakage from the drum. The drum cylinder rested on a pair of metal wheels on each side of the drum. The drum rotation speed can be adjusted to any speed between 2 and 16 rpm. Four removable inclined lifters (flights) were equally distributed around the circumference, and bolted to the inside surface of the cylinder. Flight details are shown in Figure 2. Flight length $S = 4$ cm, height $e = 2$ cm.

An electrical fan was used to provide a range of gas velocity to the drum. The velocity of the gas inlet can be varied between 1 and 3 m/s. The solids were continuously fed to the drum by a screw driver with an electronic controller.

Dense Phase Motion

Matchett and Baker[12,30] separately presented two components for the motion of particles in a cascading rotary drum dryer, air drag and dense phase motion for a sloped drum. The dense phase motion was evaluated at zero air velocity. In our study, the motion of the particles was recorded using a video camera. The observation showed that the motion of the particles in the absence of air velocity is due to hydraulic gradient over the flights, however this phenomenon was not observed when there was air flow. In the presence of air flow, the drag force on the particles forces the particles to disperse axially along the drum length, preventing solid accumulation and as a consequence preventing the hydraulic gradient over the flights. From the observations, the solid feed flow rate used in our experiments was in the range of design loading of the flight, and there was no hydraulic gradient at the lower surface of the drum.

A video camera was used to observe the starting and the finishing position of the particles as they discharge from the flights. For drum speeds <6 rpm, the particles discharge from the flights starting at an angle of $\phi < 0$ and end discharge at $\phi \geq \pi/2$. For drum speeds higher than 6–15 rpm, the discharge angle starts at $\phi > 0$ and ends at $\phi \geq \pi/2$.

Selected pictures were taken from the video of the cross section of the drum to estimate the angle of starting and finishing discharge from the flights at different drum rotation speeds. Table 1 summarises the results of the average vertical height that has been estimated from the photos compared to the height calculated from Equation (1) (through Equation (18)). The average vertical height of discharge estimated from the photos is calculated by multiplying the discharge height to diameter of the drum ratio by the actual diameter of the drum. Equation (18) calculates the average discharge height by integrating the height (Equation (1)) over the whole angles of discharges.

$$H_{ave} = \frac{\int H d\phi}{\int d\phi} = \frac{-(2r - 2h)}{\Delta\phi}(\cos\phi_f - \cos\phi_s) \quad (18)$$

where, r is the radius of the drum, h is the height of the flight, ϕ_f is the angle of finishing discharge and ϕ_s is the angle of the starting discharge. Equation (18) gives the best representation of the average vertical distance of the discharged particles from the flights.

The solid hold-up was measured experimentally to calculate the experimental residence time via Equation (19):

$$\tau = \frac{H_{up}}{F} \quad (19)$$

After steady state operation was achieved, the solid feed rate was stopped suddenly. The solids were collected at the rear of the drum at constant intervals and weighed. The solid flow rate versus time was fitted to a polynomial and integrated to determine H_{up}.

EXPERIMENTAL RESULTS AND DISCUSSIONS

A number of experiments were carried out at different gas inlet velocities [1 – 2.5 m/s] and drum rotation speeds [2 – 12 rpm] to

Table 1. Average height of discharge from the flights at different drum speeds

Drum speed	H/D ratio, start discharge (from photos)	H/D ratio, finish discharge (from photos)	Angle of start discharge	Angle of finish discharge	Average calculated by Equation (18) cm
3 rpm	0.354	0.83	$\frac{-\pi}{8}$	$\frac{5\pi}{8}$	23.4
6 rpm	0.41	0.854	$\frac{-\pi}{8}$	$\frac{5\pi}{8}$	23.4
9 rpm	0.729	0.791	$\frac{\pi}{4}$	$\frac{3\pi}{4}$	25.7
12 rpm	0.812	0.791	$\frac{\pi}{4}$	$\frac{3\pi}{4}$	25.7
15 rpm	0.833	0.812	$\frac{\pi}{4}$	$\frac{3\pi}{4}$	25.7
Average	0.627	0.721			
	0.67				
Calculated by H/D ratio			0.67×37 cm $= 24.8$ cm		
Calculated by Equation (1)			23.1 cm		
Calculated by Equation (18)			24.7		

study the effect of these two variables and also to evaluate the model. The experiments have been repeated twice and the average was applied with typical error in the residence times of 5–8%.

Effect of Air Velocity

It has been shown that increasing the inlet gas velocity has a significant impact on the residence time of the particles inside the drum. The rise of the velocity from 1 to 2.5 m/s at 6 rpm resulted in an 85% decrease in the residence time. This is clearly showing the effect of drag force on the axial advance in particle motion. The same trends have been predicted for the other settings of drum rotation speed of 3, 9, and 12 rpm as shown in Figure 4. The experimental data shows a good agreement with the model predictions with an overall absolute error of 7–10%. The low percentage of error shows the importance of the particles drag in the calculation of residence time. In a study by Lisboa et al.,[31] it is shown that Perry and Green's and Fiedman and Marshall's equations did not represent well the experimental data. They found that only Saeman and Mitchell's equation had good matches with the experimental data because it takes the particles dragging into consideration.

The axial displacement of the particle through the drum as predicted by the model is linearly proportional to the gas inlet velocity. For example, an increase in air velocity from 1 to 2.5 m/s results in a 10 cm increase in the axial motion of the particle during each fall from the flight. These results have not been reported elsewhere, it is unique to this paper due to the presence of the particles falling number (N).

Effect of Drum Speed

Experiments at variable drum speeds of 3–12 rpm were carried out at a constant inlet gas velocity to illustrate the effect of drum rotation speed. As the rotation of the rotary drum increases, the falling number of the particles (N) will increase leading to an increase in the contact time with the inlet gas. The increase in the contact time between the particles and the inlet drying medium will increase the particles' travelling distance with each fall. It is well known that the cascade rate is function of the rotational speed.[32] However, the residence time can be reduced threefold (for example at air velocity 1 m/s) as shown in Figure 5 the effect of the rotation of the drum is limited. As the rotation of the drum gets closer to the falling velocity of the particles, the number of times the particles fall will approach a fixed number. This is because a particle cannot be lifted again by the flight unless it reaches the lower surface of the drum. Data for other settings of air velocities (1.5, 2.0 and 2.5 m/s) have shown similar trends, illustrated in Figure 5.

The experimental measurement of the residence times at a variety of inlet gas velocities and along a range of rotation speeds showed good agreement with the model prediction and achieved an overall absolute error of 7% to 10%.

As expected, the falling number of the particles also predicted by the model, increases as the rotation speed of the drum increases. However, the falling number will reach a maximum point; this point is reached when the speed of drum is equal to or higher than the terminal velocity of the particles. After the maximum point, the trends are expected to become constant as illustrated in Figure 6. The maximum falling number (if centrifugation is neglected, imaginary) as predicted by the model for the circumstances of the experiments is when the rotation speed is 276 rpm or higher. At this speed the terminal velocity of the particles (5.35 m/s) is equal to the rotation speed giving a maximum number of falling of 0.59/s. These results also have not been reported elsewhere, it is unique to this paper due to the presence of the particles falling number (N).

Effect of Particle Size

Langrish et al.[29] estimated the residence time of sand with different particle sizes (195, 1315 and 5040 μm). These particle sizes were mixed at different percentages (0–100%). The particle size was found to have a very little effect compared with the large effect for the gas velocity (0–5.4 m/s). Figure 7 shows a comparison that has been made between the experimental results of Langrish with the predictions of the new model for averaged particle size of 867 μm (40% fine particle 195 μm with 60% 1315 μm coarse sand). The comparison with the experimental data shows good agreement with an average absolute error of $<10\%$. However, it should be noted that the experimental results published by Langrish et al. were for a drum which was inclined by 1° and the sand used was a mixture of different particle sizes.

Effect of Solid Flow Rate

The new model was evaluated for different solid flow rates using experimental data by Song et al.[1] Both the experimental and the model results show similar trends, illustrated in Figure 8. It is obvious

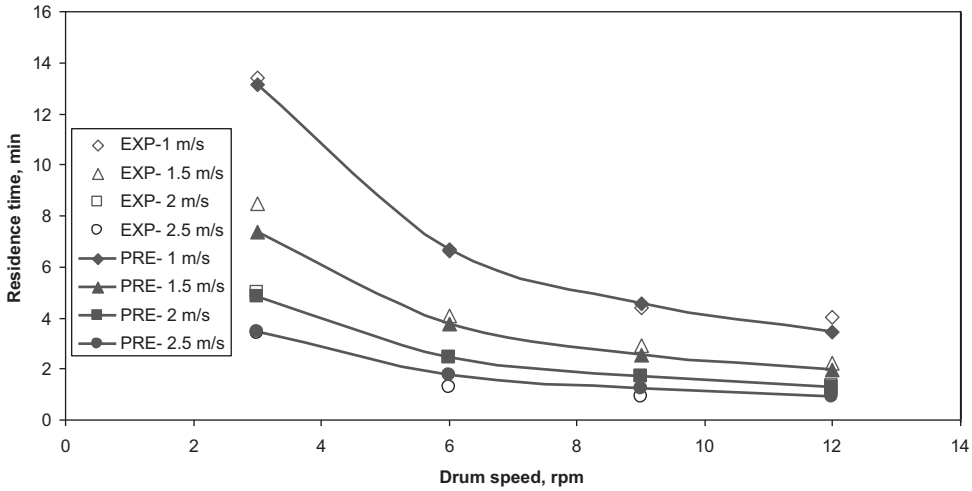

Figure 5. Comparison of the experimental results of this study with the suggested model versus rotary drum speed at variable gas inlet velocity, $D = 0.37$ m, dp = 385 μm, $L = 3.0$ m, $F_N = 4$, $F = 1$ kg/min.

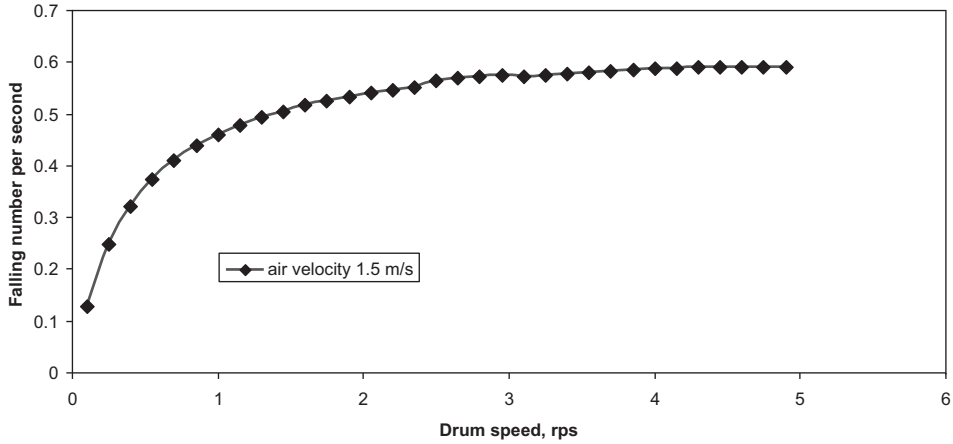

Figure 6. Number of falling of each particle for variable rotary drum rotation as predicted by the Model, $D = 0.37$ m, dp = 385 μm, $L = 3.0$ m, $F_N = 4$, $F = 1$ kg/min.

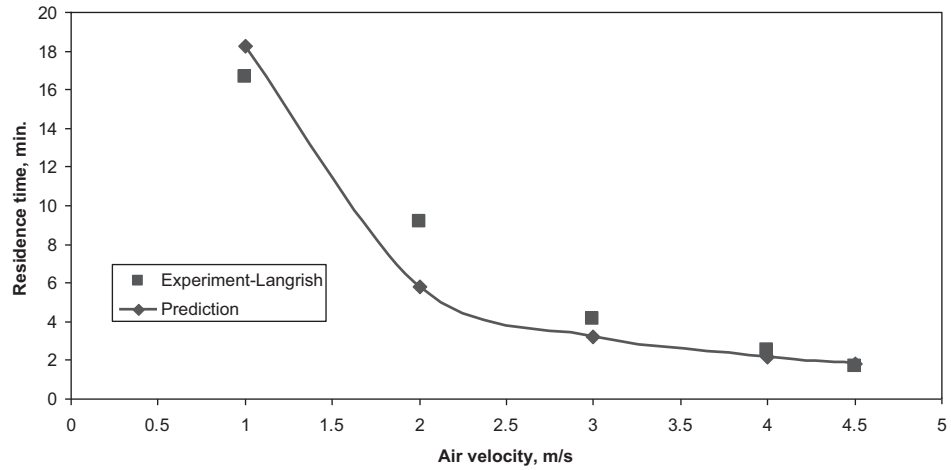

Figure 7. Comparison of the experimental results of Langrish study with the suggested model, rpm = 5, $D = 0.237$ m, dp = 867 μm, $L = 2.2$ m, $F_N = 4$, $F = 0.00717$ kg/s, slope = 1°.

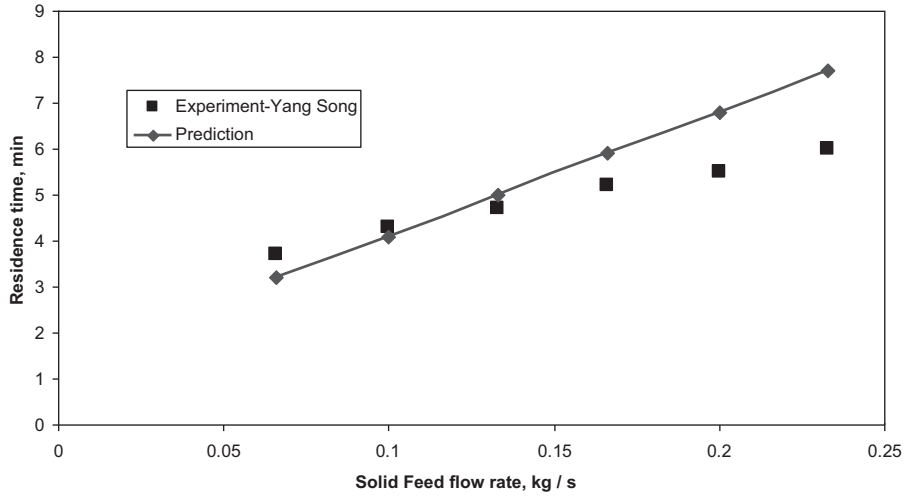

Figure 8. Comparison of the experimental results of Yang Song study with the suggested model for different feed mass flow rate, rpm = 8, $D = 0.0.305$ m, dp = 444 μm, $L = 3.05$ m, $F_N = 9$, slope = 1°.

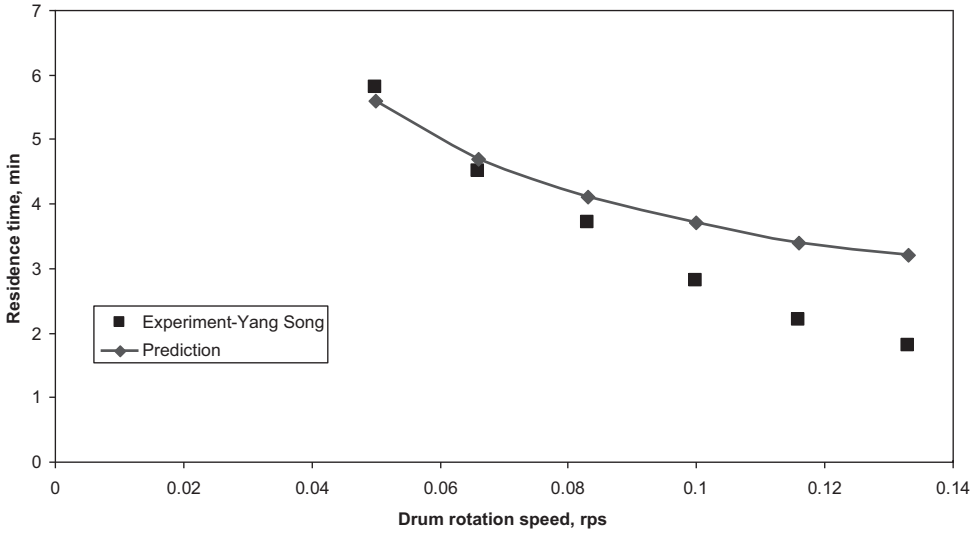

Figure 9. Comparison of the experimental results of Yang Song et al. (2003) with the model (Equation 14) for different drum rotation speeds, feed rate = 0.0855 kg/s, D = 0.0.305 m, dp = 444 μm, L = 3.05 m, F_N = 9, slope = 1°.

from Figure 8 as the feed flow rate increases the average residence time increases. As explained by Song et al.,[1] for a small amount of solid feed, the drag force exerted on the particles by the flowing gas is more pronounced. The effect of the flowing gas decreases progressively as the solid flow rate increases because the gas will be in contact with a larger quantity of solids and the gas will not able to impact the same momentum to the cascading particles. These results could also illustrate, as the flow rate of the solid increases the probability of falling of the particles decreases and gives preference to kiln action. Despite the good match between the experimental data and the data predicted from the model for the solid flow rates between 0.05 and 0.2 kg/s with an absolute error of <8%, the discrepancy increases to an absolute error of 21% for solid feed rates above 0.2 kg/s. The high error could be a result of the kiln motion because the experimental data was taken from a pilot scale rotary drum with a slope of 1° while the model was constructed for a zero slope drum. This concept is in agreement with the findings of Kelly and O'Donnell,[20] who found that the increase in solid feed rate may lead to increase in kiln action.

Figure 9 is another example of the influence of kiln action at high drum rotation speeds. However the model shows better agreement with the experimental data (from Song et al.[1]) at low rotation speeds of the drum, the discrepancy increases as the rotation of the drum increases. The experimental data gives lower residence time than the model prediction at high speed due to the kiln action as a result of the drum slope. The absolute error for the first three readings of the drum speed is around 6% compared to 50% for the final three.

Rest and Equilibrium Residence Time Calculation

Drying processes are the main objective for a rotary drum. The most important variable for drying in a rotary drum is not the mean residence time (τ), but the time spent by the particles in contact with the gas medium (τ_{contact}).[33,34] As has been shown by many researchers[35,36] the duration of drying is a fundamental variable in the drying process. The model was built to give this property via Equation (15) and the rest or equilibrium residence time (τ_{rest}) via Equation (16)

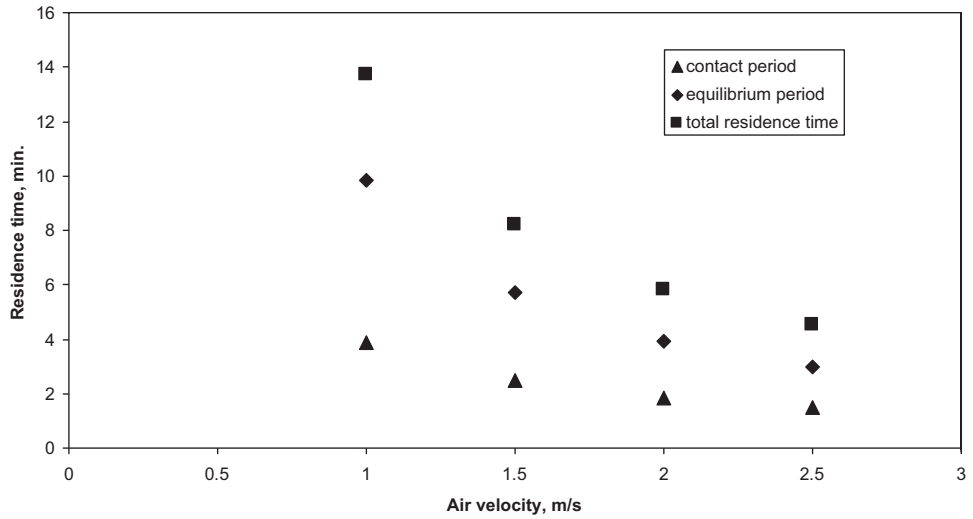

Figure 10. Average mean residence time, drying residence time, and equilibrium residence time for variable gas inlet velocity as predicted by the Model, rpm = 3, D = 0.37 m, dp = 385 μm, L = 3.0 m, F_N = 4, F = 1 kg/min.

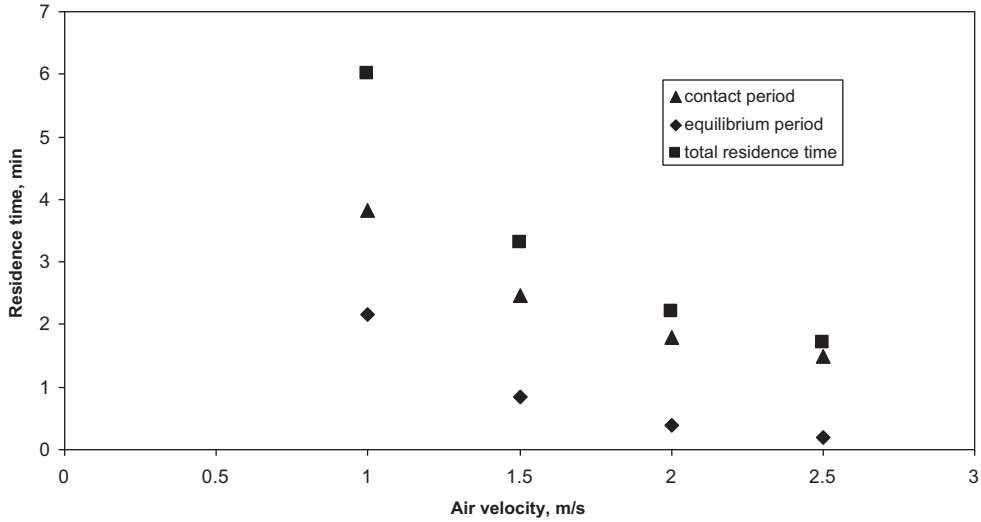

Figure 11. Average mean residence time, Drying residence time, and Equilibrium residence time for variable gas inlet velocity as predicted by the Model, rpm = 6, $D = 0.37$ m, dp = 385 μm, $L = 3.0$ m, $F_N = 4$, $F = 1$ kg/min.

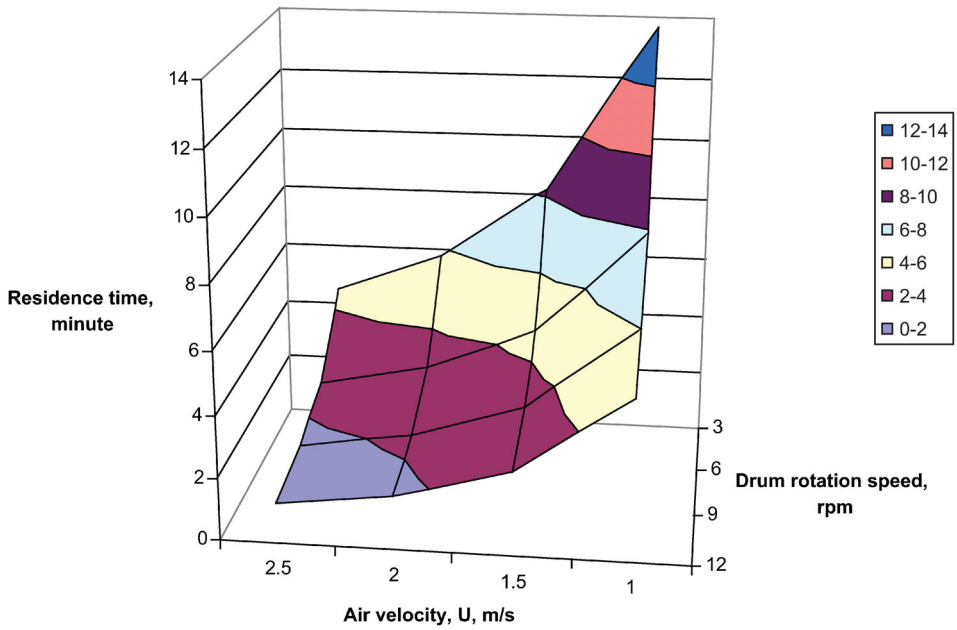

Figure 12. Three dimension plot for two variables: air velocity and drum rotation speed with the total residence time.

considering the effect of air velocity. Figure 10 shows that for the drum rotation of 3 rpm, the time spent by the particles in rest or equilibrium is approximately double the time of contact. However, when the speed of the drum is doubled to 6 rpm as shown in Figure 11, the period of contact is significantly increased, but at the same time, the mean residence time is decreased. As the gas velocity increases, the contact period gets closer to the total mean residence time of the drum and the resting time of the particle approaches the minimum. An optimum period of contact should be found through controlling both the drum speed and the gas inlet velocity. Figure 12 summarises both effects of the inlet gas velocity and the drum rotation speed on the total residence time. These results are unique to this paper due to the presence of two residence times, the residence time of contact and the residence time of rest.

CONCLUSION

The difficulty of modelling the particle transport in a rotary drum is the many major variables that are to be considered. This new model has included most of these variables such as drum rotation speed, gas inlet velocity, solid feed flow rate, falling number, number of flights, drum diameter, drum length, mass hold-up and particle properties. The most important finding of this paper is the particles' falling number. The model was able to predict important parameters for a drying process such as the mean residence time, the contact residence time and the resting or equilibrium residence

time. The model showed good agreement with the experimental data generated in this research and that borrowed from literatures with an absolute error of <10%. However, the new model did not match well when the feed rate was above 0.2 kg/s and the rotation speed was above 5 rpm, the results were good in all other cases. Further work in regards the loading rate and the kilning action of solids is required.

NOMENCLATURE

A_p	projected area of sphere shape particle, m^2
C_D	drag coefficient
D	drum diameter, m
d_p	particle diameter, μm
d_{pE}	particle diameter used in the calculation, μm
F	solid feed flow rate, kg/s
F_N	number of flights
g	gravity acceleration
h	maximum high of solid in the drum, m
H	average length of fall, m
H_{up}	solid hold-up, kg
L	length of the drum, m
m_p	particle weight, kg
N	number of falling
rps	speed of the drum, rotation per second
rpm	speed of the drum, rotation per minute
Re	particle Renold number
u	superficial inlet gas velocity, m/s
V_{ts}	particle terminal velocity, m/s
v_p	axial particle velocity, m/s
x	axial displacement, m
ρ_g	density of inlet gas, kg/m^3
ρ_p	density of the particles, kg/m^3
ρ_b	bulk density of particles in the drum, kg/m^3
ϑ	the angle of solid dispersion as viewed from the drum centre
θ	rotary drum slope
μ_g	viscosity of the inlet gas, kg/m.s
Δt	time interval, s
τ	average mean residence time, s
τ_{drying}	average mean residence time of drying, s
$\tau_{equilibrium}$	average mean residence time of equilibrium, s

APPENDIX

The actual vertical height that the particles travel when it starts falling to reach the lower surface of the drum has been estimated through videoing experiments. Photos from the video were analysed for different drum rotation speed [3–15 rpm] with constant air velocity of 2 m/s and solid feeding of 1 kg/min.

The ratio of the height of the flight when start in and finishing discharge of the particles to the drum diameter was determined.

DRUM SPEED; 3 RPM

Ratio of the height of flight when start discharge to the drum diameter:

$$\frac{H}{D} = \frac{1.7\,\text{cm}}{4.8\,\text{cm}} = 0.354$$

Ratio of the height of the flight when finish discharge to the drum diameter:

$$\frac{H}{D} = \frac{4}{4.8\,\text{cm}} = 0.83$$

Start discharge

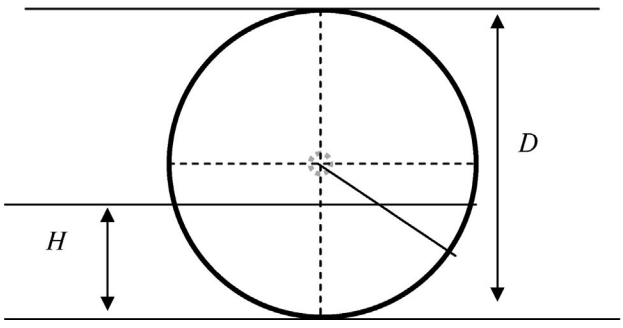

Finish discharge

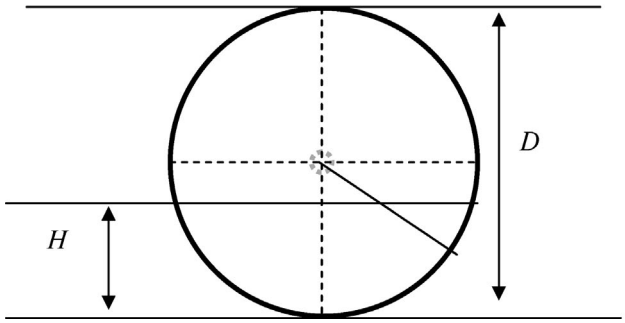

DRUM SPEED; 6 RPM

Start discharge

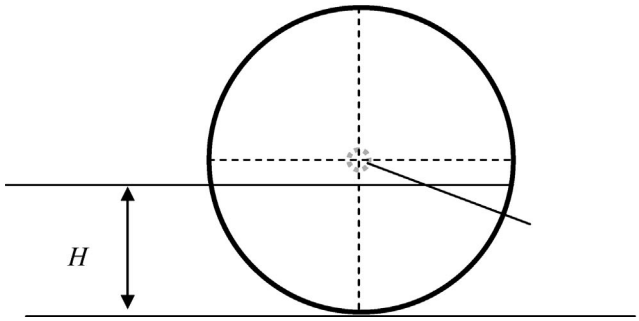

Finish discharge

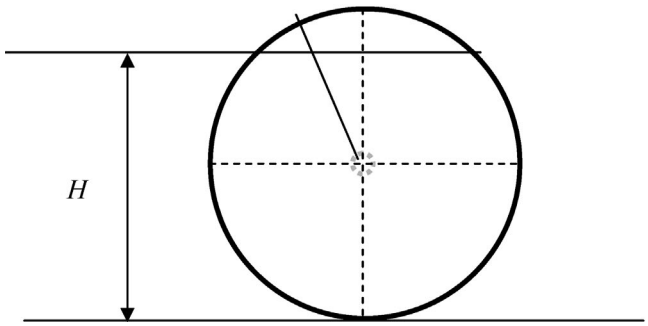

DRUM SPEED; 9 RPM

Start discharge

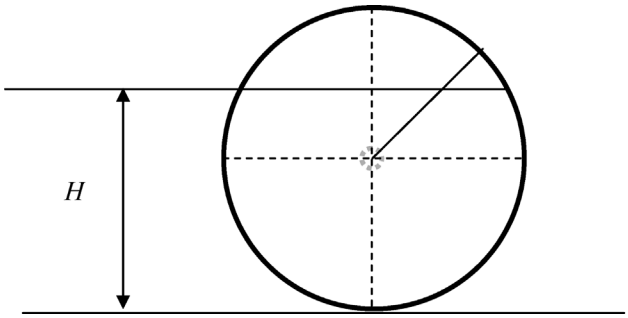

Finish discharge

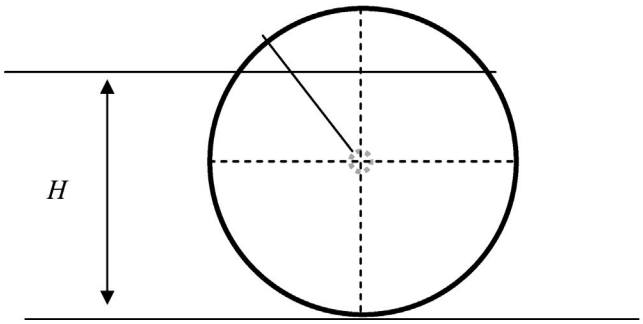

DRUM SPEED; 12 RPM

Start discharge

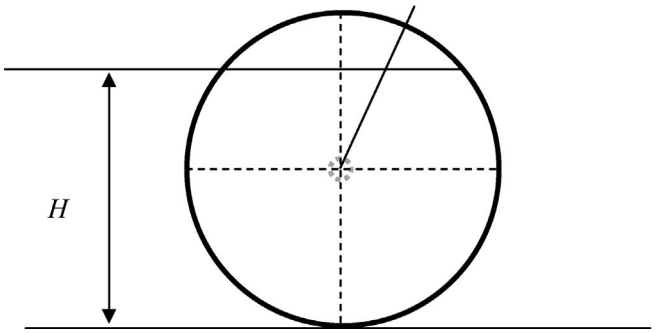

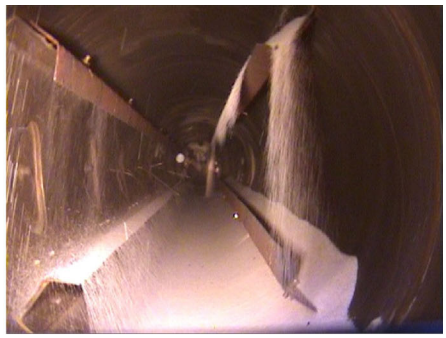

Finish discharge

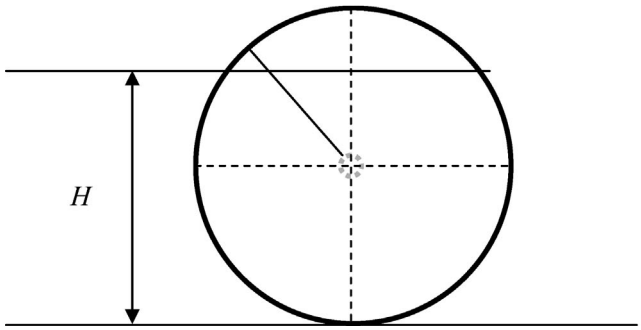

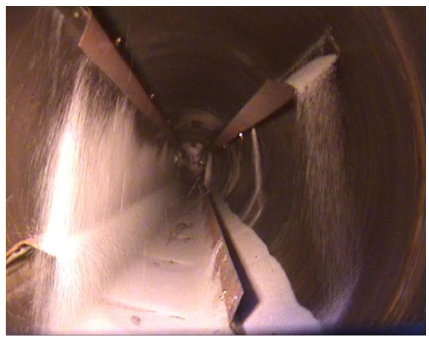

DRUM SPEED; 15 RPM

Start discharge

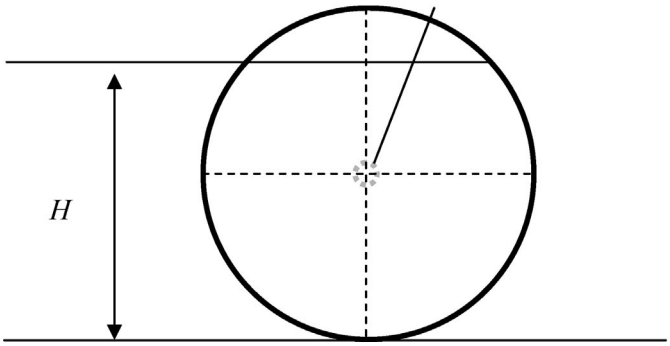

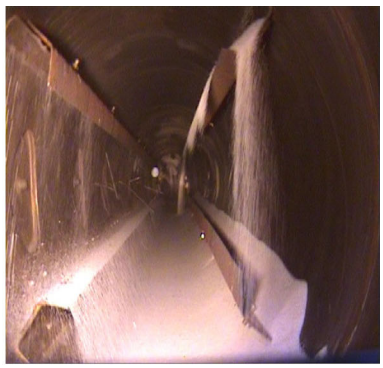

Finish discharge

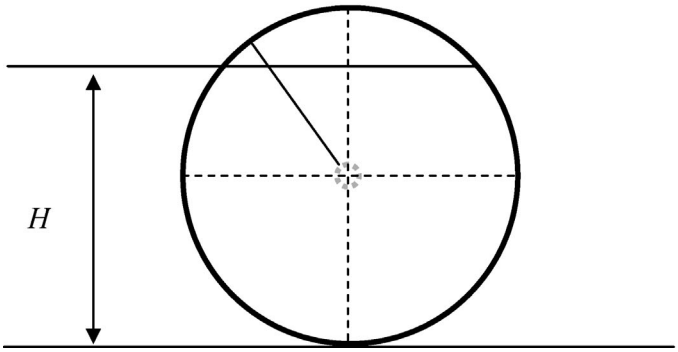

REFERENCES

[1] Y. Song, J. Thibault, T. Kurda, *Drying Technol.* **2003**, *21*, 755.

[2] R. H. Perry, D. Green, *Perry's Chemical Engineers' Handbook*, McGraw-Hill, New York **1984**.

[3] A. S. Foust, L. A. Wenzel, C. W. Clump, L. Maus, L. B. Andersen, *Principle of Unit Operations*, Wiley, New York **1960**.

[4] S. J. Friedman, J. R. Marshal, *Chem. Eng. Prog.* **1949**, *45*, 482.

[5] M. Renaud, J. Thaibault, A. Trusiak, *Drying Technol.* **2000**, *18*, 843.

[6] C. Duchesne, J. Thaibault, C. Bazin, *Ind. Chem. Res.* **1969**, *35*, 2334.

[7] J. D. Sullivan, R. T. Bui, *Can. J. Chem. Eng.* **1990**, *68*, 61,

[8] P. S. T. Sai, G. D. Surender, A. D. Damodaran, V. Suresh, Z. G. Philip, K. Sankaran, *Metall. Trans. B.* **1990**, *21B*, 1005.

[9] P. I. Alvarez, C. Shene, *Drying Technol.* **1994**, *12*, 1629.

[10] S. Shahhosseini, *Drying modelling and control of rotary drying process*, PhD Thesis, Department of Chemical Eng. University of Queensland, **1998**.

[11] I. C. Kemp, Proceeding of the 14th International Drying Symposium (IDS 2004); B, 790.

[12] A. J. Matchett, C. G. J. Baker, *J. Sep. Process Technol.* **1988**, *9*, 5–13.

[13] W. F. Cao, T. A. G. Langrish, *Drying Technol.* **1999**, *17*, 825.

[14] J. J. Kelly, P. O'Donnell, *Trans. I. Chem. Eng.* **1977**, *55*, 243.

[15] C. G. J. Baker, *Drying Technol.* **1992**, *10*, 365.

[16] F. Y. Wang, I. T. Cameron, J. D. Lister, V. Rudolph, Proceeding of the 9th International Drying Symposium, **1994**, 1327.

[17] N. Earner, *The effect of air flow on the movement of solids in rotary drums*, Bachelor of Eng. Thesis, University of Queensland, **1994**.

[18] M. E. Sheehan, P. F. Britton, P. A. Schneider, *Chem. Eng. Sci.* **2005**, *60*, 4171.

[19] P. F. Britton, M. E. Sheehan, P. A. Schneider, *Powder Technol.* **2006**, *165*, 153.

[20] J. J. Kelly, J. P. O'Donnell, *Encyclopaedia of Chemical Technology*, 3rd edition, John Wiley and Sons, New York **1981**, 8.

[21] A. S. Mujumdar, *Handbook of Industrial Drying*, 3rd edition, Taylor & Francis Group, Florida, USA **2006**.

[22] J. P. Pan, T. J. Wang, J. J. Yao, Y. Jin, *Powder Technol.* **2006**, *162*, 50.

[23] J. J. Kelly, J. P. O'Donnell, *I. Chem. Symp.* Series. **1978**, *29*, 38.

[24] J. H. Vincent, *Aerosol Sampling: Science, Standards, Instrumentation and Application*, John Wiley & Sons, Ltd., Chichester, England **2007**.

[25] O. Koichiro, K. Hidehiro, F. Katsuya, T. Yuji, *Trans. Jpn. Soc. Mech. Eng.* **2004**, *70*, 1965.

[26] C. Wardjiman, A. Lee, M. E. Shehan, M. Rhodes, *Powder Technol.* **2008**, *188*, 110.

[27] A. Lee, *Modeling the solid transport phenomena within flighted rotary dryers*, PhD Thesis, James Cook University, **2008**.

[28] E. Mauret, M. Renaud, *Chem. Eng. Sci.* **1997**, *52*, 1819.

[29] T. A. G. Langrish, S. E. Papadakis, C. G. J. Baker, *Drying Technol.* **2002**, *20*, 325.

[30] A. J. Matchett, C. G. J. Baker, *J. Sep. Process Technol.* **1987**, *8*, 11.

[31] M. H. Lisboa, A. B. Alves, D. S. Vitorino, W. B. Delaiba, J. R. D. Finzer, M. A. S. Barrozo, *Braz. J. Chem. Eng.* **2007**, *24*, 365.

[32] L. Yliniemi, *Advanced control of a rotary dryer*. Academic Dissertation presented to the Faculty of Technology, University of Oulu, Finland **1999**.

[33] I. Hamawand, Modelling of drying under superheated steam. 7th Asia–Pacific Drying Conference (ADC 2011) Tianjin, China, 18–20 September 2011.

[34] I. Hamawand, *Int. J. Eng.* **2011**, *24*, 119.

[35] A. Al-Kassir, J. Ganan, F. V. Tinaut, *Appl. Therm. Eng.* **2005**, *25*, 2816.

[36] J. F. Gonzalez, B. Ledesma, A. Alkassir, J. Gonzalez, *Biomass Bioenergy* **2011**, *35*, 4399.

Manuscript received January 3, 2013; revised manuscript received February 24, 2013; accepted for publication March 4, 2013.